International Journal of Safety and Security Engineering
Vol. 16, No. 10, October, 2026, pp. 2429-2437
Journal homepage: http://iieta.org/journals/ijsse

Optimized Ultrasonic Transducer Configuration of Flow Velocity Vector Measurement for Leakage Point Identification

Jirayut Hansot[1], Wongsakorn Wongsaroj[1,2], Natee Thong-Un[1,2*], Hiroshige Kikura[3]

[1] Department of Instrumentation and Electrical Energy Engineering, King Mongkut's University of Technology North Bangkok, Bangkok 10800, Thailand
[2] Center of Excellence on Instrumentation Technology and Automation, King Mongkut's University of Technology North Bangkok, Bangkok 10800, Thailand
[3] Laboratory for Zero-Carbon Energy, Institute of Science Tokyo, Tokyo 152-8550, Japan

Corresponding Author Email: natee.t@eng.kmutnb.ac.th

Copyright: ©2026 The authors. This article is published by IIETA and is licensed under the CC BY 4.0 license (http://creativecommons.org/licenses/by/4.0/).

https://doi.org/10.18280/ijsse.161019

Received: 22 August 2026
Revised: 29 September 2026
Accepted: 26 October 2026
Available online: 31 October 2026

Keywords:
ultrasonic, velocity vector, leakage detection

ABSTRACT

Nowadays, in several industries, liquid leakage occurs probably during accident circumstances in the process. This event is able to injure plant operators, nearby humans, and harm the environment when it leaks out of the container or vessel. A measurement technique that is able to identify the leakage location is necessary. This paper presents an ultrasonic measurement technique with an optimized transducer configuration to obtain the flow velocity vector profiles for visualizing the leakage point in the liquid container. The measurement system employs an ultrasonic transducer with one emitter and two receivers, and a multiple channel pulser/receiver. The ultrasonic velocity profiler (UVP) and vector reconstruction formula is used as the measurement algorithm. The transducers' configuration, including the gap distance between emitter and receiver, and angle installation of the receiver, is adjusted to make an accurate measurement result. The experimental demonstration was executed in the rectangular water tank that leakage location was simulated. The velocity vector profile was derived reasonably via the utilization of an optimized transducer configuration, which was able to estimate the leakage location.

1. INTRODUCTION

In industrial processes, such as liquid tanks, vessels, or pond, the leakage of liquid can occur in abnormal condition of the process or during accidence. In a chemical plant [1], if the chemical or toxic liquid leaks to outside, consequence to be harmful to humans, any creatures, and the environment. Also, in nuclear industry, after accidents such as Fukushima accident, the commissioning task has been essential to remove fuel debris in the reactor. The leakage of contaminated water distributed in the vessel owing to internal structure damage also was huge issue [2, 3]. The water that leakages outside of the vessel is able to cause disease to humans and affect to environment for a long time due to its radioactivity.

Therefore, the measurement system that is collaborated with the mobile robot has been required for identifying the leakage point of the liquid distributed in the tank, vessel, or pond occurred in these accidents. The measurement system has to survive in the liquid that is poor visibility, toxic or even high radioactive.

Ultrasonic velocity profiler (UVP) is basically applied to measure the velocity distribution of the liquid [4]. The technique is based on echography method. This technique is a non-invasive measurement. The measurement result derived has high time-spatial resolution. It has been applied to several liquids even in opaque conditions or harsh environments such as water, liquid sodium, liquid metal, magnetic liquid, and so on [5-8]. The ultrasonic transducer can withstand radioactively instinctively and able to work in chemical or corrosive liquid. So, the UVP has a chance to apply for leakage estimation in the any liquids in the accident circumstances. However, it has been basically for one-dimensional velocity profile measurement. Therefore, the measurement system has to be modified in order to obtain multi-dimensional or vector velocity for leakage estimation.

A low-cost ultrasonic method for locating liquid leaks uses a single transducer and a compact set of instruments [9]. A robotic arm rotates the transducer through a small angle to acquire measurements from different directions, allowing the flow velocity vector to be reconstructed and the leak location to be visualized. Accurate localization depends on precise control of the arm's motion. Multiple transducers can provide measurements from different directions without rotating a single probe, although the additional hardware may increase the cost.

Multi-transducer configurations have been used to measure 3D velocity vectors in open-channel flow with one transmitter and four receivers [10] and 2D velocity vectors with a UVP comprising one transceiver and one receiver [11]. A compact five-element transducer connected to a five-channel

pulser/receiver has also been used to measure 3D flow velocity vectors in a horizontal pipe. The same configuration supports 2D measurements [12].

Ultrasonic phased array technology has been applied in several fields, such as the detection of material defects in metals [13-15] and composite materials [16], as well as in the medical field [17]. For liquid leakage detection, phased array transducer works with multiple channel pulser/receiver was applied to estimate water leakage points in the tank [18-20]. The transducer immersed into the liquid to obtain the 2D velocity vector profile of the liquid, the vector velocity magnitude and direction can identify the location of the leakage point.

However, these developments had not been completed to investigate transducer configuration such as gap distance between emitter and receiver, and angle installation of receiver which has probably affected the measurement quality.

This research presents the investigation of the transducer configuration and demonstrates the optimized configuration of the transducers for velocity vector measurement and liquid leakage estimation respectively. This work focuses on two-dimensional measurement. The experiment was conducted in water tank that the leakage location simulated. The selected configuration was applied for experimental measurement of the measurement system to identify the leakage point. Moreover, the performance evaluation was executed.

2. ULTRASONIC VELOCITY PROFILER FOR VELOCITY PROFILE MEASUREMENT

2.1 Ultrasonic velocity profiler basic

The UVP technique is based on ultrasonic reflection concept. Figure 1 shows the basic principle of the UVP. The ultrasonic pulse is emitted from the transducer into the liquid dispersed with small particles. The small particle is assumed to have its motion follow the liquid streamline as the stroke number of the relation between liquid and particle is lower than 0.1. The ultrasonic wave is reflected from the moving particle to the same transducer. The wave is emitted repeatedly to the particle, the echo signals is reflected consequently, Doppler signal affected by moving particle is demodulated from repetition of the echo obtained. Velocity V of the moving particle can be derived as substitution the Doppler frequency f_D into Eq. (1). If several small particles are dispersed in the liquid, the velocity profile $V(i)$ of the liquid can be obtained which i is measurement channel.

$$V(i) = \frac{c f_D(i)}{2 f_0} \tag{1}$$

where, c is sound velocity and f_0 represents basic frequency of ultrasonic wave.

Figure 2 illustrates the pulse repetition technique utilized to demodulate the Doppler signal from echo signals reflected by small particles that move from position 1 to position 6. The echo signals $e(t)$ derived along with repetition time of emitting is represented in Eq. (2), where $t_{\mathrm{n,i}}$ represents the delay time of the echo at n$^{\mathrm{th}}$ pulse repetition and channel i, $A_{\mathrm{n,i}}$ is the signal amplitude of the echo at n$^{\mathrm{th}}$ pulse repetition and channel i. The phase shift of echo signals occurs. Then, the echo signals are multiplied by cosine and sine function and filtered by a low-pass filter to remove the carrier wave component of basic frequency. Therefore, the Doppler signal $D_i(n)$ in each measurement channel can be extracted from the echo signals as expressed in Eqs. (3)-(5). Doppler frequency can be estimated by the FFT, autocorrelation and so on. This work used autocorrelation as frequency estimator [21].

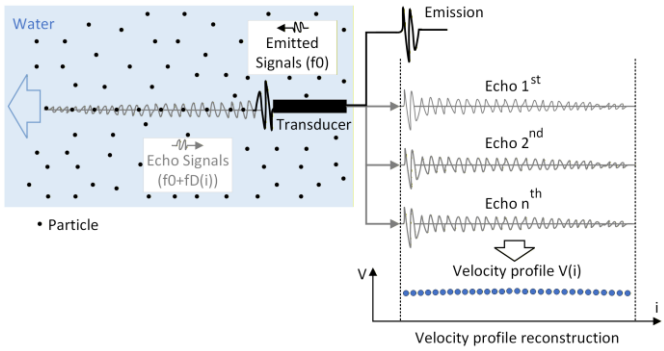


Figure 1. Ultrasonic velocity profiler (UVP) principle for velocity profile measurement

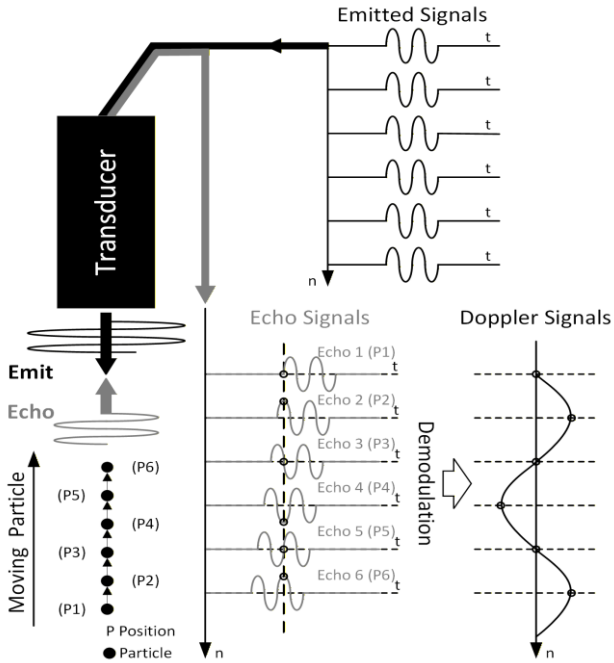


Figure 2. Pulse repetition technique

$$e(t) = \sum_{n=0}^{N_{\mathrm{REP}}-1} A_{n,i} \cos 2\pi \left[f_0 (t - t_{n,i}) + n \frac{f_{\mathrm{D},i}}{f_{\mathrm{PRF}}} \right] \tag{2}$$

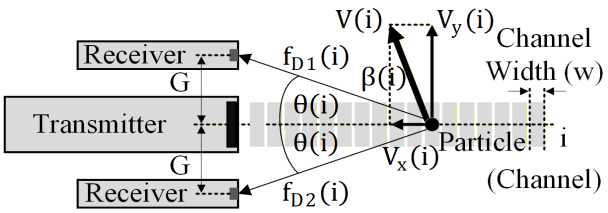
$$D_i(t) = \{ 2e(t) \mathrm{e}^{j2\pi f_0 t} \}_{\mathrm{LOWPASS}} \tag{3}$$

$$\begin{aligned} D_i(t) = & \sum_{n=0}^{N_{\mathrm{REP}}-1} A_{n,i} \cos 2\pi \left(\frac{f_{\mathrm{D},i} n}{f_{\mathrm{PRF}}} - f_0 t_{n,i} \right) \\ & -j \sum_{n=0}^{N_{\mathrm{REP}}-1} A_{n,i} \sin 2\pi \left(\frac{f_{\mathrm{D},i} n}{f_{\mathrm{PRF}}} - f_0 t_{n,i} \right) \end{aligned} \tag{4}$$

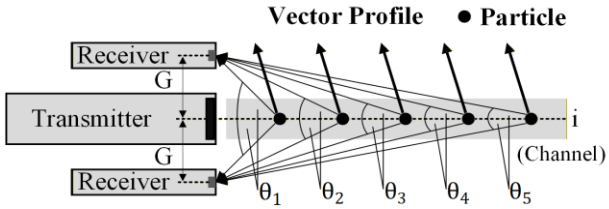
$$\begin{aligned} D_i(n) = & A_{n,i} \cos \left(\frac{2\pi n f_{\mathrm{D},i}}{f_{\mathrm{PRF}}} - \emptyset_i \right) \\ & -j A_{n,i} \sin \left(\frac{2\pi n f_{\mathrm{D},i}}{f_{\mathrm{PRF}}} - \emptyset_i \right) \end{aligned} \tag{5}$$

2.2 Velocity vector measurement with multiple transducers

Figure 3 shows transducer configuration for the velocity vector measurement, this work focusses on two dimensional. The set of transducer consist of one emitter and two receivers. The emitter emits the ultrasonic wave to the moving particle and echo reflected by the particle to two receivers. Virtually, the receiver 1 receives Doppler frequency $f_{D1,i}$. The receiver 2 receives Doppler frequency $f_{D2,i}$. The echo angle θ_i depends on measurement channel i, which is determined by gap distance between emitter and receiver G. Substitution of both Doppler frequency in each channel into Eqs. (6) and (7), the $V_{1,i}$ and $V_{2,i}$ can be calculated. Then, axial velocity $V_{x,i}$ and radial velocity $V_{y,i}$ are able to be computed as Eqs. (8) and (9). The velocity magnitude can be reconstruct as expressed in Eq. (10).



(a) Single particle



(b) Multi-particles

Figure 3. Velocity vector measurement with multiple transducer

$$V_{1,i} = \frac{c f_{D1,i}}{2 f_o} \tag{6}$$

$$V_{2,i} = \frac{c f_{D2,i}}{2 f_o} \tag{7}$$

$$V_{x,i} = \frac{V_{1,i} - V_{2,i}}{sin\,\theta_i} \tag{8}$$

$$V_{y,i} = \frac{V_{1,i} + V_{2,i}}{1 + cos\theta_i} \tag{9}$$

$$V_i = \sqrt{V_{x,i}^2 + V_{y,i}^2} \tag{10}$$

3. ULTRASONIC MEASUREMENT SYSTEM

In this work, the UVP measurement system employed is shown in Figure 4, consisting of multiple transducers, multi-channels pulser/receiver including digitizer in the equipment, and computer. The emitter had basic frequency 4 MHz with active diameter 5 mm. The receivers responded to 4 MHz ultrasonic wave and had special design to have small active diameter width 0.3 mm × 5 mm for receiving the echo signal with the minimum uncertainty (0.3 mm is approximate to the 4 MHz wavelength). The pulser/receiver provided 4 channels that work in pulse-echo mode. It included digitizer function with sampling rate of 50 Ms/s. The computer was utilized for UVP processing and monitoring via LabVIEW software. The UVP parameter setting is represented in Table 1.

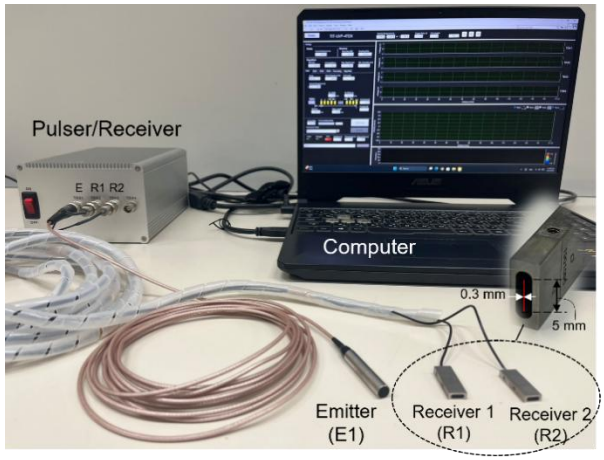


Figure 4. Ultrasonic measurement system

Table 1. Ultrasonic velocity profiler (UVP) parameter setting

Parameter	Value
Basic frequency	4 MHz
Pulse amplitude	140 Vp-p
Number of cycles	4
Pulse repetition frequency	2 kHz
Number of repetitions	128
Channel width	2.22 mm

4. EXPERIMENT FOR OPTIMIZED TRANSDUCERS CONFIGURATION

This section presents the optimization of transducers configuration, gap distance G between emitter and receiver, and angle installation α of receivers are configuration concerned as illustrated in Figure 5. The range of gap distance for investigation was between 8 mm and 20 mm. For the angle installation was set from 0 to 40 degrees. The Doppler signal demodulated from the echo signal as illustrated in Figure 6 was used for this evaluation by determining signal to noise ratio (SNR) of the signal as represented in Eq. (11).

$$SNR\ (dB) = 20 \log_{10} \frac{A_{signal}}{A_{noise}} \tag{11}$$

where, A_{signal} is Doppler signal amplitude and A_{signal} means noise amplitude on Doppler signal.

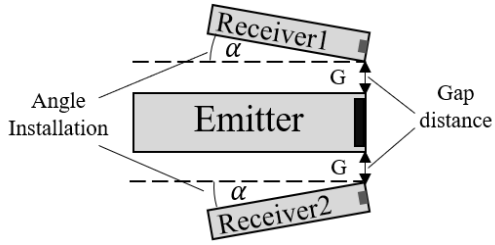


Figure 5. Transducers configuration

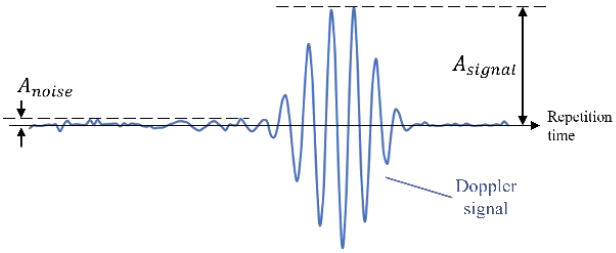
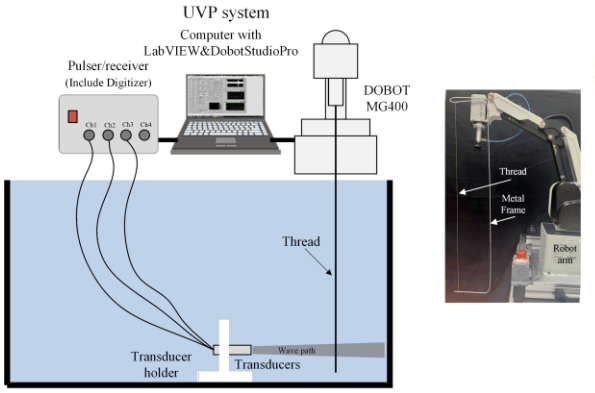
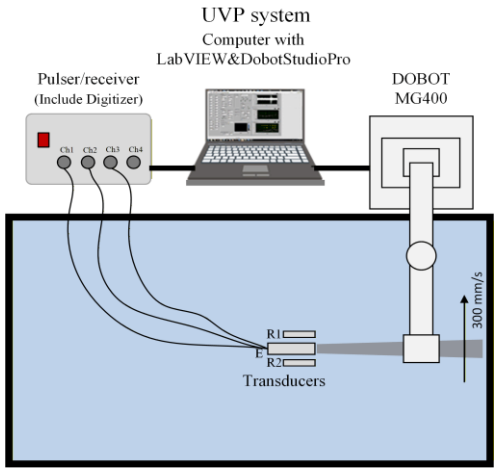


Figure 6. Example of doppler signal



(a) Side view



(b) Top view

Figure 7. Experimental setup for optimized transducer configuration

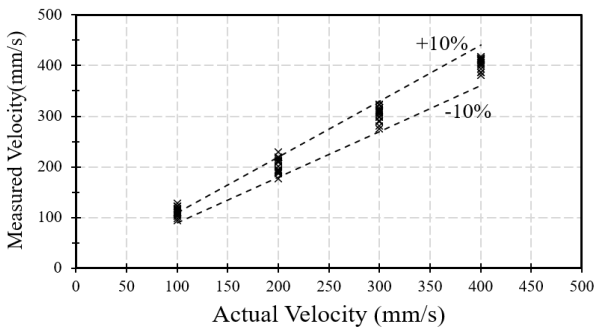


Figure 8. Result of thread moving calibration

Figure 7 illustrates the experimental setup. The UVP system explained in section 3 was used for conducting the experiment. The tap water was liquid medium. The transducers were installed on the holder and immersed in the water. The transducers connected to the pulser/receiver and computer respectively. The thin thread was stretched by the metal frame to work as small particle. It was installed with the robot arm (Brand: Dobot, Model; MG400). The movement of the robot can control the thread to pass the measurement line to generate Doppler signal. The speed of movement could be controlled via robot control software (Dobot Studio Pro). The moving speed was set at 300 mm/s. The velocity was set to a value close to the leakage flow velocity used in the experiment described in the next section. Thread moving controlled by robot arm was calibrated in several velocity points as shown in Figure 8. The result discrepancy was approaximately about ±10%. The measurement depth of testing was between 0 and 200 mm. The ranking procedure for transducer configuration selecting was based on the evaluation of the SNR in nine points of measurement depth between 0 mm and 200 mm. Which configuration that has SNR in all points higher than 10 dB was the acceptable configuration.

This threshold has been adopted in several studies for various applications, including material defect detection and medical applications. The study [22] proposed an evaluation of the error factors associated with the ultrasonic transmitted beamwidth in the measurement of myocardial minute velocity. Their study confirmed that the measurement error increased when the SNR was lower than 10 dB.

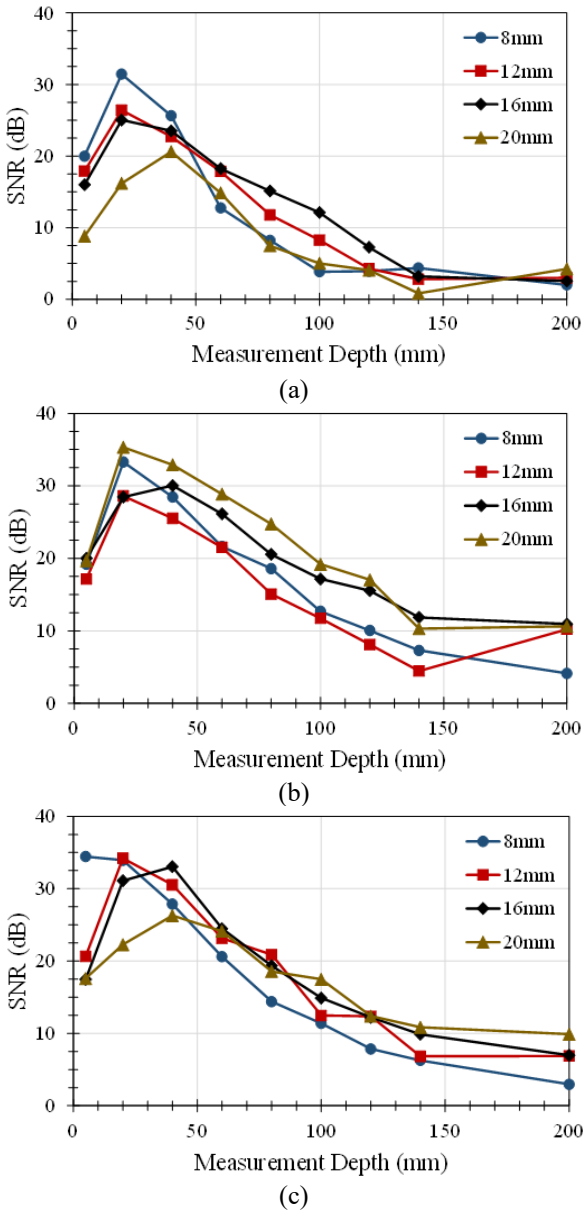
Table 2 and Figure 9 illustrate the result of testing. To keep quality of the measurement result, the SNR has to be higher than 10 dB. Figure 9(a) represents the result of the angle installation 0 degree, the SNR between 0 and 60 mm of measurement depth of all gap distance was higher than 10 dB but beyond 100 mm SNR was lower than 10 dB. As angle installation increased to 10 degrees as shown in Figure 9(b), the SNR from the measurement depth 0 to 100 mm was bigger than 10dB, beyond 100 mm of depth, SNR of only measurement gap of 16 mm and 20 mm were above 10 dB. Figure 9(c) shows the SNR of the angle installation at 20 degrees. The SNR of all gap distances obtained between measurement depth 0 and 100 mm was higher than 10 dB. However, after 120 mm of measurement depth, SNR of all gap distance was under 10 dB except of the gap at 20 mm that had SNR level approximately to above 10 dB and continue to 140 mm of measurement depth. When the angle installation was adjusted to 30 degrees as shown in Figure 9(d), the result of SNR was shown in Figure 9(d). The result of the gap distance of 12 mm, 16 mm and 20 mm has acceptable SNR until 120 mm of depth. After that, unsatisfied SNR was observed with all configurations. Lastly, the SNR of the angle installation was set at 40 degrees as represented in Figure 9(e). The result of the gap distance of 8 mm, 12 mm and 16 mm was lower than 10 dB when the measurement depth about 100 mm or before, only 20 mm of gap distance was able to has satisfied SNR until measurement depth 120 mm. Table 2 show quantitative comparison among all 20 angle–gap combinations. SNR values above 10 dB are indicated in bold.

From all results, the selected to be the acceptable configuration was at installation angle 10 degrees with the gap distance of 16 mm and 20 mm. In the other hand, the poor configuration come from installation of angle 0 degrees with gap distance of 8 mm and 20 mm and installation angle 40 degrees with gap distance of 12 mm and 8 mm.

The configuration of installation angle 10 degrees with the gap distance of 16 mm and 20 mm and installation angle 40 degrees with gap distance of 12 mm and 8 mm will be set for demonstrating to identify the leakage point and investigate their performance in next section.

Table 2. Quantitative comparison of signal to noise ratio (SNR) in each transducer configuration

Degrees (°)	Gap (mm)	Depth(mm) 5	20	40	60	80	100	120	140	200
		SNR (dB)								
0	8	**19.9**	**31.4**	**25.6**	**12.7**	8.2	3.8	3.9	4.3	2.0
	12	**17.8**	**26.4**	**22.7**	**17.8**	**11.7**	8.2	4.2	2.8	2.9
	16	**16.0**	**25.0**	**23.5**	**18.2**	**15.1**	**12.1**	7.2	3.1	2.5
	20	8.8	**16.1**	**20.6**	**14.8**	7.4	5.0	4.0	0.8	4.2
10	8	**19.1**	**33.2**	**28.4**	**21.6**	**18.5**	**12.6**	**10.0**	7.2	4.1
	12	**17.1**	**28.6**	**25.5**	**21.5**	**15.0**	**11.7**	8.1	4.4	10.2
	16	**20.0**	**28.4**	**30.0**	**26.1**	**20.5**	**17.1**	**15.5**	**11.8**	**10.9**
	20	**19.6**	**35.3**	**32.9**	**28.8**	**24.7**	**19.1**	**17.0**	**10.3**	**10.6**
20	8	**34.4**	**33.9**	**27.8**	**20.5**	**14.3**	**11.3**	7.8	6.2	2.9
	12	**20.6**	**34.2**	**30.5**	**23.1**	**20.8**	**12.4**	**12.3**	6.8	6.8
	16	**17.4**	**31.1**	**33.0**	**24.4**	**19.3**	**14.8**	**12.2**	9.8	6.9
	20	**17.6**	**22.2**	**26.2**	**24.1**	**18.5**	**17.4**	**12.3**	**10.8**	9.8
30	8	**31.2**	**31.2**	**20.8**	**13.6**	**10.6**	3.8	3.3	1.0	1.5
	12	**38.9**	**35.8**	**32.0**	**23.7**	**21.2**	**17.1**	**10.8**	9.2	5.4
	16	**36.9**	**34.7**	**30.7**	**23.6**	**19.3**	**15.5**	**11.9**	6.6	3.6
	20	**18.6**	**36.3**	**35.4**	**29.1**	**23.1**	**23.7**	**14.6**	7.2	11.8
40	8	**36.6**	**35.1**	**22.2**	**15.2**	9.8	5.8	4.1	4.3	0.0
	12	**33.6**	**31.8**	**23.1**	**13.3**	7.4	9.7	3.2	3.5	0.0
	16	**32.9**	**35.9**	**27.1**	**19.6**	**13.1**	6.4	4.2	2.0	0.0
	20	**34.4**	**35.2**	**33.7**	**24.3**	**19.4**	**15.9**	9.9	6.2	0.0



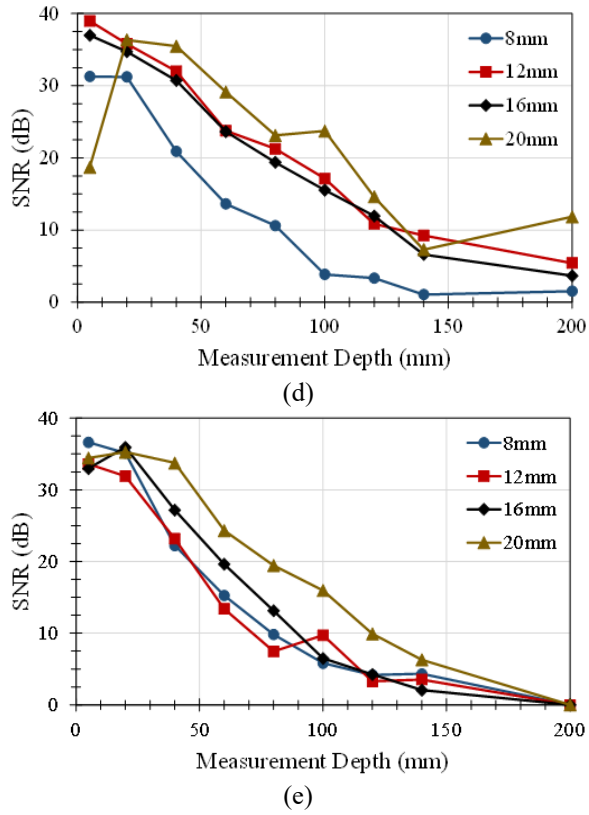


Figure 9. Result of optimized transducer configuration

5. LIQUID LEAKAGE POINT ESTIMATION

The acceptable and poor transducer configurations were selected to demonstrate the measurement of liquid leakage point. The acceptable configuration was 10 degrees angle installation with 16 and 20 mm gap distances, is called configuration A and B respectively in this experiment. In the other hand, transducers set for angle installation with 40 degrees with 8 and 12 mm of gap distance was the poor which is called configuration C and D. The demonstration was

executed by the experiment setup as shown in Figure 10. The transducers were placed at the location of x axis: 100 mm and y axis was 0 mm as represented in Figure 11; the measurement depth was 100 mm totally. The medium for the measurement was the tap water dispersed with 50 µm nylon particle work as the tracer particles. The leakage location was simulated by the hole of 32 mm connected to the pump suction. The liquid circulation flow rate was set to 18 L/min, as measured using a variable-area flow meter. Based on the hole diameter and flow rate, the calculated leakage velocity was approximately 370 mm/s.

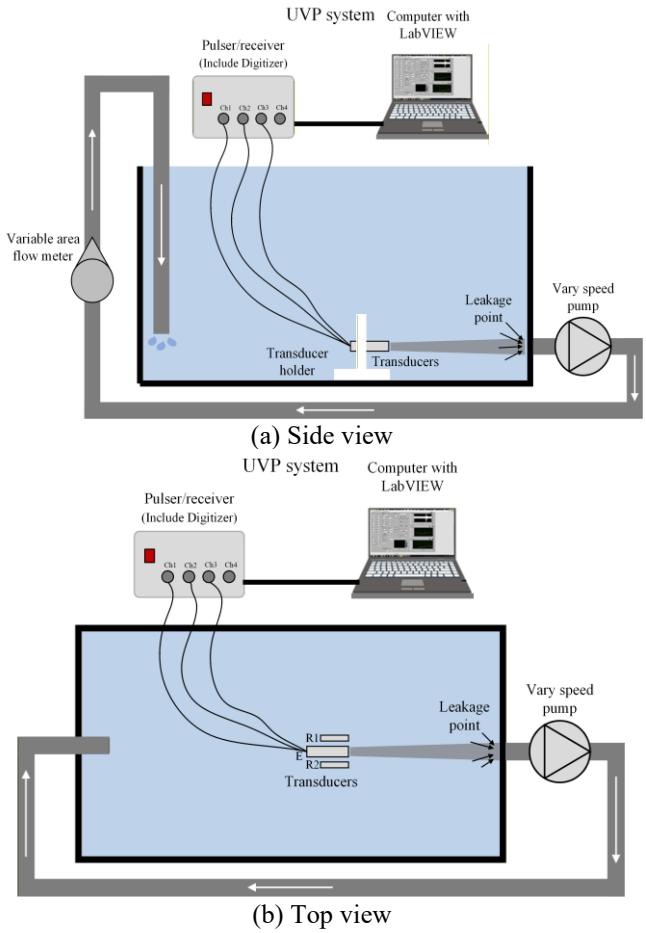


Figure 10. Experiment setup of liquid leakage point measurement

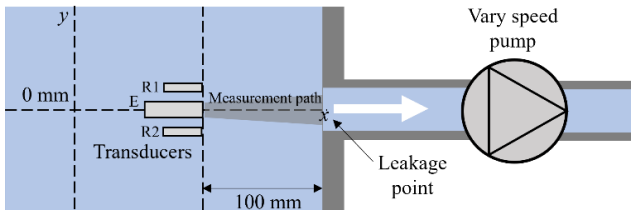
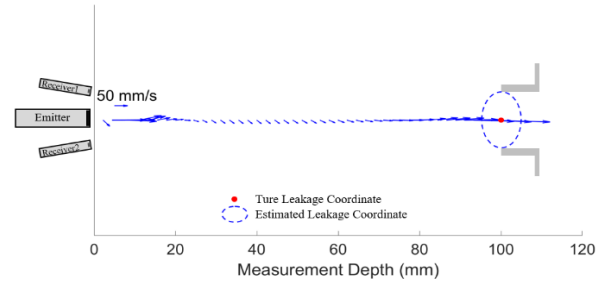
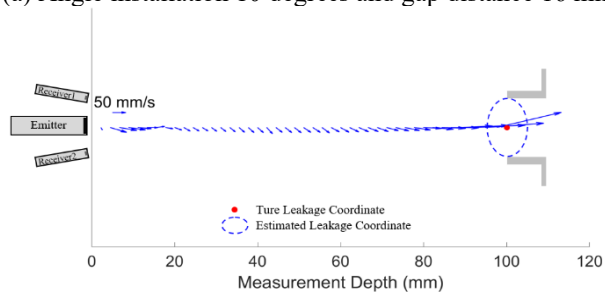


Figure 11. Transducer installation at location of x axis: 100 mm and y axis was 0 mm

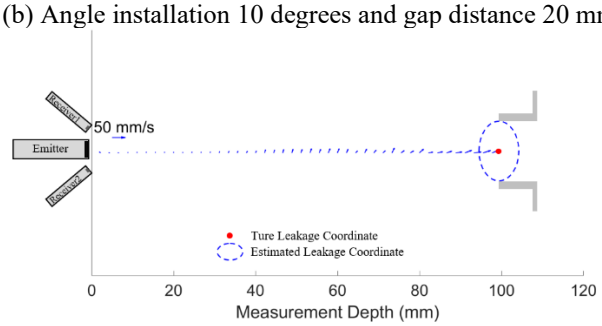
Figure 12 illustrates the measurement result obtained from four configurations. The result was averaging velocity data of the 1000 instantaneous profiles of *V1* and *V2* obtained and reconstructed follows the equation in section 2 to obtain velocity vector profile. The all results were able to show the ability of the visualization for liquid leakage point. Obvious leakage can be seen. The result measured by the configuration A and B illustrated the reasonable velocity vector when compared with the result derived from the configuration C and D which showed ambiguous vector.



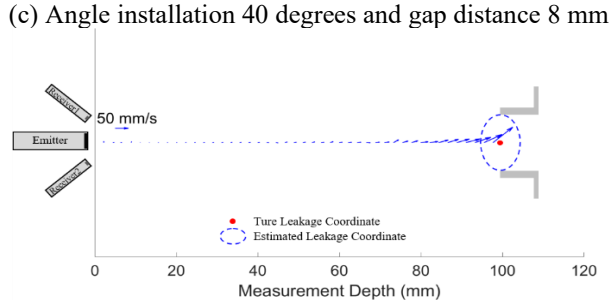
(a) Angle installation 10 degrees and gap distance 16 mm



(b) Angle installation 10 degrees and gap distance 20 mm



(c) Angle installation 40 degrees and gap distance 8 mm



(d) Angle installation 40 degrees and gap distance 12 mm

Figure 12. Measurement result of leakage point identification with transducer installation at x axis: 100 mm and y axis was 0 mm

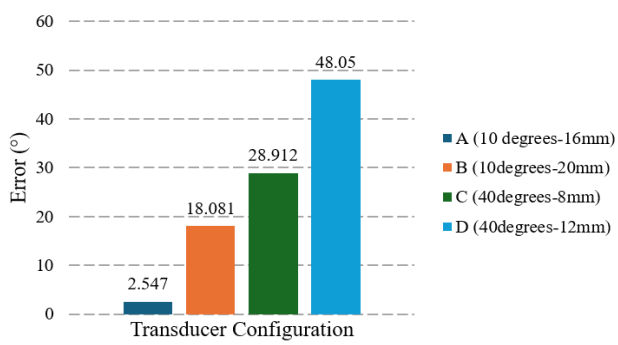


Figure 13. The directional error of the resultant vector was evaluated at a measurement depth of 98 mm, with the transducers positioned at (x = 100) mm and (y = 0) mm

Figure 13 illustrates the directional error of the resultant vector at a measurement depth of 98 mm, with the transducers positioned at (x = 100) mm and (y = 0) mm. The localization error in leakage point identification can be influenced by the measurement line resolution and the transducer active diameter, which determine the beam width. In this work, the measurement line resolution was set to 2.22 mm, and the transducer active diameter was 5 mm. Therefore, the possible localization error along the depth axis was estimated to be ±2.22 mm, while that along the lateral axis was approximately ±2.5 mm. Transducer configuration A and B provided low error obviously. Figure 14 informs the standard deviation of the instantaneous velocity data *V1* and *V2* measured by all configurations which clearly interpret measurement repeatability of configuration A and B were better than configuration C and D.

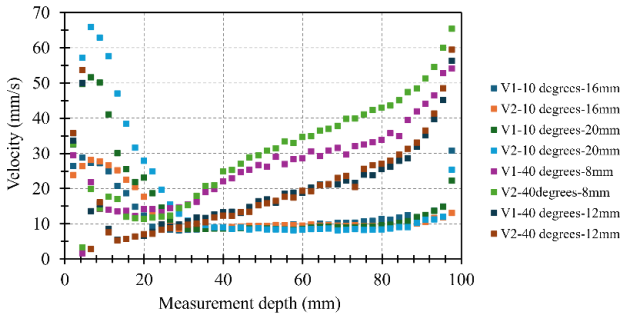
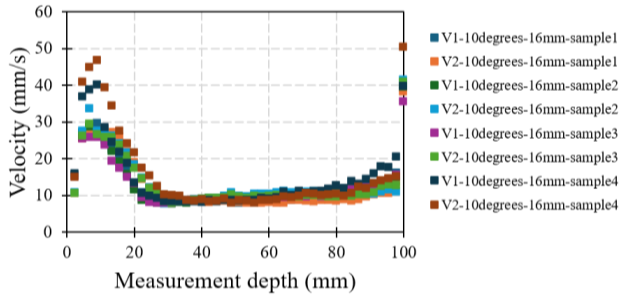
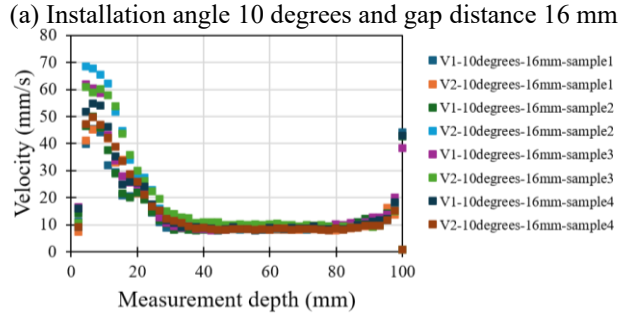


Figure 14. Standard deviation of the instantaneous velocity data *V1* and *V2* measured all configurations at location of x axis: 100 mm and y axis was 0 mm



(a) Installation angle 10 degrees and gap distance 16 mm



(b) Installation angle 10 degrees and gap distance 20 mm

Figure 15. Standard deviation of the instantaneous velocity data *V1* and *V2* measured of configurations A and B at location of x axis: 100 mm and y axis was 0 mm with 4 sample of 500 instantaneous profiles

Figure 15 represents the standard deviation of four samples of 500 instantaneous velocity data *V1* and *V2* measured of configurations A and B at location of x axis: 100 mm and y axis was 0 mm in order to confirm the repeatability of the measurement. For this expeiment, multi-channels pulser/receiver including digitizer in the equipment, and computer was restarted before measurement in each sample was conducted. Information in the figure identifies the measurement had good repeatability.

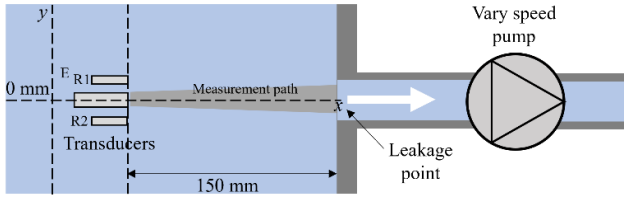
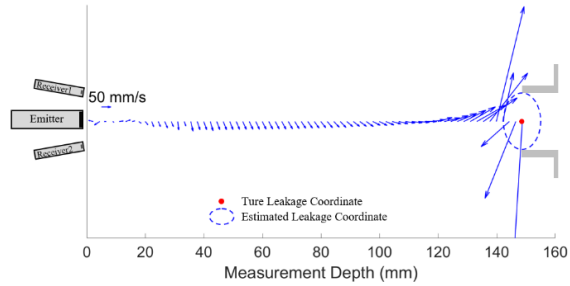
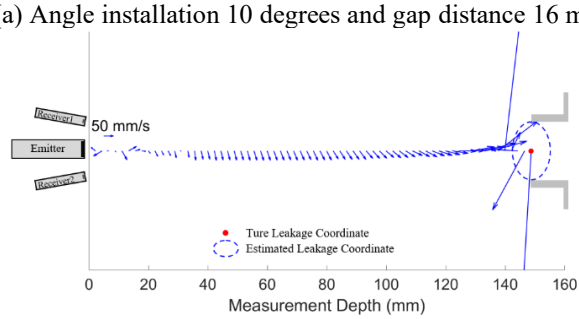


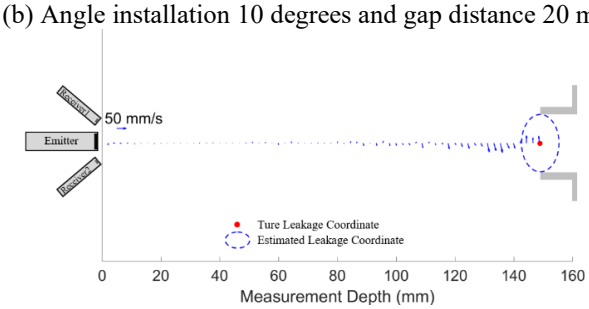
Figure 16. Transducer installation at location of x axis: 150 mm and y axis was 0 mm



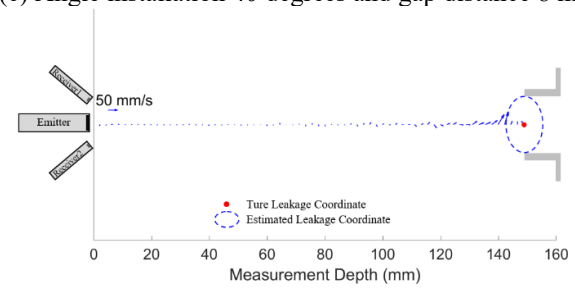
(a) Angle installation 10 degrees and gap distance 16 mm



(b) Angle installation 10 degrees and gap distance 20 mm



(c) Angle installation 40 degrees and gap distance 8 mm



(d) Angle installation 40 degrees and gap distance 12 mm

Figure 17. Measurement result of leakage point identification with transducer installation at x axis: 150 mm and y axis was 0 mm

Next, the experiment was conducted by placing transducers at the location of x axis: 150 mm and y axis was still 0 mm as shown in Figure 16, the measurement depth was totally 150 mm. The result informs the ability of measurement beyond the

measurement depth at 100 mm. The result of each configuration is shown in Figure 17. The configuration A and B were still having applicability to identify the leakage location but were not good of accuracy due to the small echo angle and the SNR close to 10 dB at far region near to 150 mm of measurement depth. Also, the averaging measurement data had high standard deviation in all measurement depth as illustrated in Figure 18. Besides, for the configuration C and B, there was not the possibility of measurement.

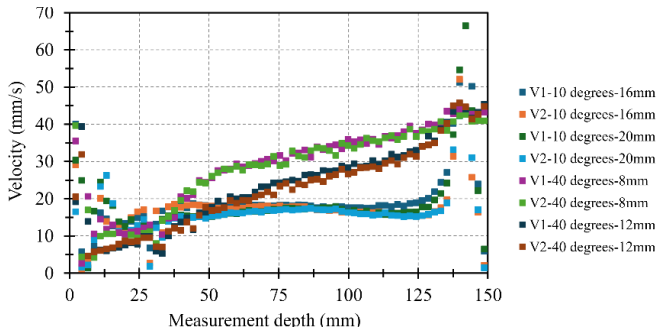


Figure 18. Standard deviation of the instantaneous velocity data *V1* and *V2* measured of all configurations at location of x axis: 150 mm and y axis was 0 mm

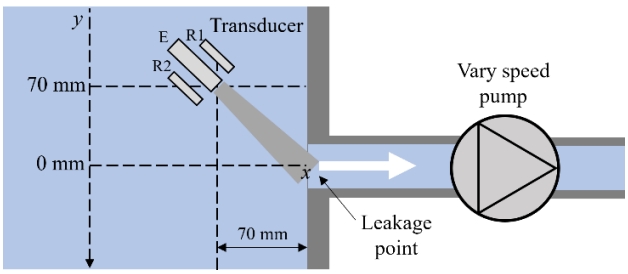
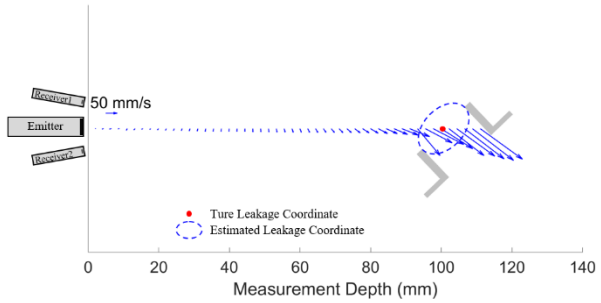
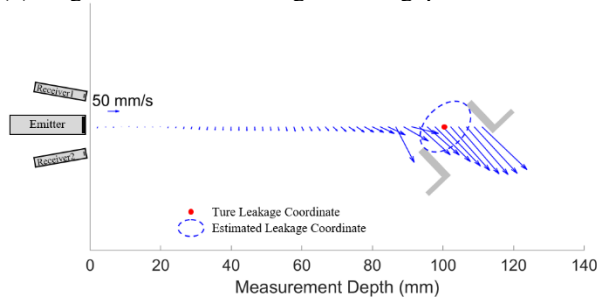


Figure 19. Transducer installation at location of x axis: 70 mm and y axis was 70 mm



(a) Angle installation 10 degrees and gap distance 16 mm



(b) Angle installation 10 degrees and gap distance 20 mm

Figure 20. Measurement result of leakage point identification with transducer installation at x axis: 70 mm and y axis was 70 mm

Then, the measurement was conducted to find the leakage point by putting transducers at location of x axis: 70 mm and y axis was 70 mm as represented in Figure 19. Configuration A and B were employed for this demonstration. The velocity vector result can point to the leakage point obviously as shown in Figure 20.

6. CONCLUSION

This work proposed the ultrasonic measurement to obtain two-dimensional velocity vector profile which is designed to identify the liquid leakage location. Multiple transducers consisted of one emitter and two receivers, and multi-channel pulser/receiver were employed. The UVP processing was programmed via LabVIEW software. The optimization of transducer configuration was executed experimentally both transducer gap distance and installation angle. The gap distance at 16 mm and 20 mm on angle installation of 10 degrees provided the acceptable configuration of the demonstration. Then, the experiment of liquid leakage identification was conducted by utilizing the acceptable and poor transducer configuration. The results were compared and were able to point out that the acceptable configuration provided better result than the poor configuration. The research strongly recommend that optimization of transducer configuration was essential process of making the ultrasonic measurement for velocity vector profile measurement as well as identifying liquid leakage point.

The present study focused on evaluating the feasibility of the proposed multi-element UVP method under controlled experimental conditions. Therefore, several parameters were kept constant to minimize the influence of additional variables on the measured velocity profiles. Our future work will focus on investigating the effects of different leakage flow rates and leakage hole sizes on the measurement results. The influence of leakage direction and different transducer positions should also be examined in greater detail. Further experiments using liquids with different properties and tracer particle concentrations are needed to evaluate their effects on signal quality. The effects of boundary reflections should also be considered, as reflected ultrasonic waves may influence the received signals. Measurements at different depths should be performed to evaluate the performance of the proposed method over a wider measurement range. These additional studies will help further assess the robustness and practical applicability of the proposed method.

ACKNOWLEDGMENT

This research was supported through equipment provided by the collaboration of Institute of Science Tokyo, Japan and King Mongkut's University of Technology North Bangkok, Thailand.

REFERENCES

[1] Ghasem, N., Henda, R. (2008). Principles of Chemical Engineering Processes, 1st ed. CRC Press. https://doi.org/10.1201/b16323

[2] Lahey, R.T., Moody, F.J. (1993). The Thermal-Hydraulics of a Boiling Water Nuclear Reactor, 2nd ed.

La Grange Park, Ill., USA: American Nuclear Society.
[3] Tokyo Electric Power Company Holdings Corporation. (2019). Progress of medium and long-term roadmap. http://www.tepco.co.jp/decommission/information/committee/roadmap_progress/pdf/2019/d191219_05-j.pdf.
[4] Takeda, Y. (1986). Velocity profile measurement by ultrasound Doppler shift method. International Journal of Heat and Fluid Flow, 7(4): 313-318. https://doi.org/10.1016/0142-727X(86)90011-1
[5] Takeda, Y. (1991). Development of an ultrasound velocity profile monitor. Nuclear Engineering and Design, 126(2): 277-284. https://doi.org/10.1016/0029-5493(91)90117-Z
[6] Kikuchi, K., Takeda, Y., Obayashi, H., Tezuka, M., Sato, H. (2006). Measurement of LBE flow velocity profile by UDVP. Journal of Nuclear Materials, 356(1-3): 273-279. https://doi.org/10.1016/j.jnucmat.2006.05.028
[7] Kikura, H., Takeda, Y., Durst, F. (1999). Velocity profile measurement of the Taylor vortex flow of a magnetic fluid using the ultrasonic Doppler method. Experiments in Fluids, 26(3): 208-214. https://doi.org/10.1007/s003480050281
[8] Eckert, S., Gerbeth, G. (2002). Velocity measurements in liquid sodium by means of ultrasound Doppler velocimetry. Experiments in Fluids, 32(5): 542-546. https://doi.org/10.1007/s00348-001-0380-9
[9] Hurther, D., Lemmin, U. (1998). A constant-beam-width transducer for 3D acoustic Doppler profile measurements in open-channel flows. Measurement Science and Technology, 9(10): 1706-1714. https://doi.org/10.1088/0957-0233/9/10/010
[10] Wongsaroj, W., Thong-un, N., Hansot, J., Treenuson, W., Chanwutitum, J., Kikura, H. (2025). Low-cost ultrasonic measurement for estimation of liquid leakage point. Journal of Mechanical Science and Technology, 39(1): 249-258. https://doi.org/10.1007/s12206-024-1224-4
[11] Obayashi, H., Tasaka, Y., Kon, S., Takeda, Y. (2008). Velocity vector profile measurement using multiple ultrasonic transducers. Flow Measurement and Instrumentation, 19(3-4): 189-195. https://doi.org/10.1016/j.flowmeasinst.2007.11.007
[12] Shoji, N., Kikura, H., Takahashi, H., Wongsaroj, W. (2022). Three-dimensional velocity distribution measurement using ultrasonic velocity profiler with developed transducer. Journal of Flow Control, Measurement & Visualization, 10(1): 32-55. https://doi.org/10.4236/jfcmv.2022.101003
[13] Kim, Y., Cho, S., Park, I.K. (2021). Analysis of flaw detection sensitivity of phased array ultrasonics in austenitic steel welds according to inspection conditions. Sensors, 21(1): 242. https://doi.org/10.3390/s21010242
[14] Wang, H., Fan, Z., Chen, X., Cheng, J., Chen, W., Wang, Z., Bu, Y. (2022). Automated classification of pipeline defects from ultrasonic phased array total focusing method imaging. Energies, 15(21): 8272. https://doi.org/10.3390/en15218272
[15] Lee, J., Chia, C.C., Lee, J.R. (2026). Weld defect classification in phased-array ultrasonic testing using a CNN with FiLM layer. International Journal of Aeronautical and Space Sciences. https://doi.org/10.1007/s42405-026-01251-2
[16] Yuan, C., Xie, C., Li, L., Zhang, F., Gubanski, S.M. (2016). Ultrasonic phased array detection of internal defects in composite insulators. IEEE Transactions on Dielectrics and Electrical Insulation, 23(1): 525-531. https://doi.org/10.1109/TDEI.2015.005225
[17] Lee, W., Roh, Y. (2017). Ultrasonic transducers for medical diagnostic imaging. Biomedical Engineering Letters, 7(2): 91-97. https://doi.org/10.1007/s13534-017-0021-8
[18] Kikura, H., Ihara, T., Kawachi, T. (2015). Study on ultrasonic measurement for determination of leakage from reactor vessel and debris inspection. In The 11th National Conference on Nuclear Science and Technology. Agenda and Abstracts, Da Nang, Vietnam. https://inis.iaea.org/records/38hda-4tc28.
[19] Nishiwaki, R., Hamdani, A., Takahashi, H., Endo, G., Kikura, H. (2018). Development of a remote water leakage localization system combined with phased array UVP and robot. In 11th International Symposium on Ultrasonic Doppler Methods for Fluid Mechanics and Fluid Engineering, Berlin, Germany, pp. 88-91.
[20] Kawachi, T., Takahashi, H., Kikura, H. (2018). A study on 2-D vector flow mapping by echo-PIV with total focusing method. In Advances in Fluid Mechanics XII, WIT Transactions on Engineering Sciences, pp. 275-286. https://doi.org/10.2495/AFM180281
[21] Kasai, C., Namekawa, K., Koyano, A., Omoto, R. (1985). Real-time two-dimensional blood flow imaging using an autocorrelation technique. IEEE Transactions on Sonics and Ultrasonics, 32(3): 458-464. https://doi.org/10.1109/T-SU.1985.31615
[22] Sugahara, K., Mori, S., Arakawa, M., Kanai, H. (2021). Evaluation of error factors depending on ultrasonic transmitted beamwidth in measurement of myocardial minute velocity. Japanese Journal of Applied Physics, 60(SD): SDDE05. https://doi.org/10.35848/1347-4065/abef0e